Multiscale Analysis on Electrical Properties of Carbon Fiber-Reinforced Wood Composites

Xiaolong Zhu and Liping Sun *

Carbon fiber was selected as a reinforcement for the manufacture of composite materials. Electrical properties of carbon fiber reinforced wood composites (CFRWCs) were studied by multiscale analysis, which is an all-rounded method to analyze CFRWCs from the macroscopic area to the microcosmic field. It was found that the insulated wood fiber materials could conduct electricity after adding a certain proportion of carbon fibers. The dielectric constants and the capacitances of CFRWCs increased gradually with increasing carbon fiber content in the composites from 55 wt.% to 75 wt.% when a certain condition prevails. However, the loss tangents and the surface resistivities of CFRWCs decreased as the carbon fiber content was increased continuously. The data of surface resistivity represented a negative growth situation with increasing temperature from 20 °C to 120 °C and exhibited a negative temperature coefficient (NTC) effect. The movement of electrons was also analyzed due to temperature rise.

Keywords: CFRWCs; Multiscale; Electrical properties; Atomic dynamics

*Contact information: College of Mechanical and Electrical Engineering, Northeast Forestry University, Harbin 150040 China; *Corresponding author: zdhslp@163.com*

INTRODUCTION

As a renewable resource, wood has been widely used in various fields, in which it can be used to form new composites with special microstructures and properties by adding other raw materials (Lee 2010). Besides, the price of wood is quite low, which is beneficial to reduce the cost of production. However, the electrical resistance value of wood is extremely high. It has been shown that the resistance value of wood can reach $2 \times 10^{10}\ \Omega$ when the percentage of moisture is 7% (Diao and Sun 1993).

Carbon fibers have shown outstanding results in research related to multi-functional composites. It is well known that composites with negative temperature coefficient (NTC) effect play a significant role in the electrical properties. Carbon fibers and carbon nanofibers, as the most important reinforcements, are widely employed in composites (He 2010). In addition, they have many features, such as high electrical conductivity (Bal 2010; Al-Saleh *et al*. 2013; Chawla *et al*. 2013), good mechanical properties (Al-Saleh and Sundararaj 2011), and low thermal expansivity (Chen and Ting 2002; Poveda *et al*. 2012; Khan *et al*. 2013).

The number of dissertations dealing with multiscale composites has increased in recent years, especially for carbon fibers reinforced composites (Alexopoulos *et al*. 2010; Lee *et al*. 2011; Rodriguez *et al*. 2011). In France, Salinier *et al*. (2013) studied the electrical properties of multiscale composite materials based on multiwalled carbon nanotubes. They concluded that conductive fiber content and space distribution have a direct influence on the conductivity of composites. Poveda and Gupta *et al*. (2014)

concluded that the high dielectric constant was related to high capacitance at the low frequency by studying electrical properties of carbon reinforced composites. Compared with previous analysis methods, multiscale analysis can study the electrical properties of composites from not only resistance value, but also atom structure.

Carbon fiber reinforced wood composites (CFRWCs) exhibit both good electrical properties and NTC effect. When the concentration of carbon fiber becomes high enough to be in the percolation region, the conductivity of composites will increase by orders of magnitude with the slight addition of fiber content (Yang *et al*. 2000). Besides, electrical properties will also change, including the dielectric constant, loss tangent, capacitance, and surface resistivity. Preparation methods of composite materials are the foundation of developing electrical properties. It has been shown that carbon fiber content, stirring method, temperature, and humidity all can directly impact the electrical properties of composites (Wang *et al*. 2009). Based on the above factors, in order to study the electrical properties of CFRWCs from the macroscopic area to the microcosmic field, carbon fiber content and temperature were chosen as the main variables in the present work.

EXPERIMENTAL

Materials

Main raw materials

The short-cut carbon fibers used for this study were obtained from Hangzhou High-teach Composite Material Co., Ltd. (China). The purity of the carbon fibers was 95.0%. The density and the tensile modulus of carbon fibers were 1.5 g/cm^3 and 200 GPa, respectively. Polar wood fibers were acquired from Qingdao From-wood New Energy Equipment Co., Ltd. (China), the length of which was about 3 mm.

Other chemicals

Acetone, isocyanate resin, urea-formaldehyde resin, and ammonia chloride were used for composites production. Acetone with a density of 0.788 g/cm^3 was added to the 50 wt.% isocyanate resin, which was used as adhesive. Urea-formaldehyde resin mixed with ammonia chloride was used to solidify wood fibers.

Methods

The carbon fibers were dispersed, and then stirred with addition of the mixture of acetone and isocyanate resin at 20 °C for 10 min. The isocyanate resin/acetone ratio was 1/2 by weight. Such a mixture ratio could ensure that the mixture works well. The main role of acetone was as a good solvent for isocyanate resin, and it could dilute isocyanate resin. Isocyanate resin as adhesive has a stable performance of chemical properties and hardly conducts electricity, so it has been reported to have no impact on electrical properties of composites (Gui 2011). The poplar wood fibers were air-dried in the open air for 24 h. After that, ammonia chloride was first required to diluted to 20 wt.% by water, which was added to the 48.5 wt.% urea-formaldehyde resin. Then the solution was mixed into the poplar wood fibers.

Certain proportions of carbon fibers and poplar wood fibers were put into a mechanical mixer with a speed range of 100 to 2000 rpm for stirring. Isocyanate resin contained isocyanate groups, which set off chemical reactions with hydroxyl and moisture of fiber, and then formed covalent bonds and polyurea. These resultants promoted adherence between fibers. In this experiment, the mixture was stirred at 1500 rpm for 30 min, which ensured that carbon fibers mixed uniformly with wood fibers. The mixture ratios of wood fibers and carbon fibers are shown in Table 1.

Table 1. Composition of Carbon Fibers/Wood Fibers

Composites	Carbon Fibers (wt.%)	Wood Fibers (wt.%)
Single-sided Samples	55	45
	65	35
	75	25
Two-sided Samples	55	45
	65	35
	75	25
Crude Wood Sample	0	100

The mixture was covered on the bottom surface or both the top and the bottom surfaces of a mold to form single-sided samples or two-sided samples. Meanwhile, the other space of the mold was filled with poplar wood fibers. The length and the thickness of the mold was 420 mm by 420 mm and 12 mm, respectively. After that, the mould was placed in a preforming press for 5 min. Finally, the mixed materials were compressed in the thermocompressor for 10 min at 190 °C and 4.5 MPa after prepressing. Under the high temperature, the effect of isocyanate resin and urea-formaldehyde resin would be promoted, which is beneficial to bond and solidify the fibers between each other. The bonding between wood fiber and carbon fiber would also be enhanced. Figure 1 shows the images of CFRWCs samples. Due to the hydrophobicity of carbon fiber, adhesion between reinforcements and wood fibers, to some extent, was decreased. After the high-temperature process, the surface of carbon fibers would tend to become rougher, thus strengthening the structural integration between carbon fibers and wood fibers.

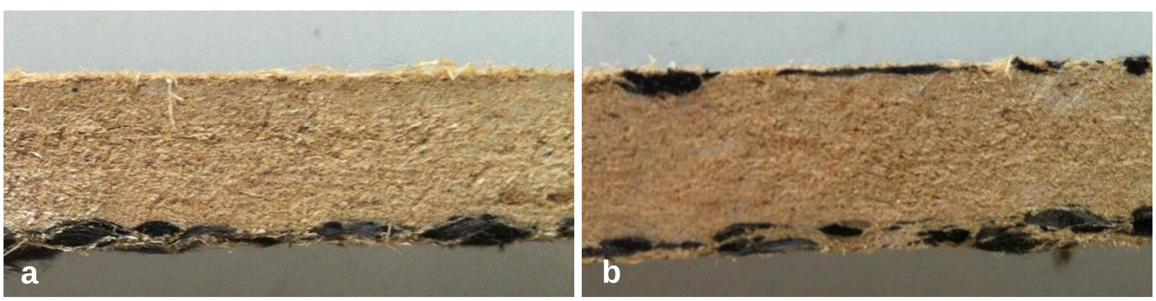

Fig. 1. Images of CFRWCs samples: (a) single-sided CFRWCs board; and (b) two-sided CFRWCs board

Sample boards dimensions were 100 mm × 50 mm × 12 mm. Each sample was labeled as follows: (1) Single-sided samples of CFRWCs contained 55 wt.%, 65 wt.%, and 75 wt.% carbon fibers, which were numbered as $11^{\#}$, $12^{\#}$, and $13^{\#}$, respectively; (2) Double-sided samples of CFRWCs contained 55 wt.%, 65 wt.%, and 75 wt.% carbon fibers , which were numbered as $21^{\#}$, $22^{\#}$, and $23^{\#}$, respectively; and (3) Crude wood samples contained 100 wt.% wood fibers, which were numbered as $31^{\#}$. In order to reduce the effects of random experimental deviations, the number of each labeled item was three. The value of each labeled item was the average value of samples containing both the same content and form, and then was listed in the table below.

Measurement of mechanical properties

Carbon fiber-reinforced wood composites were mainly manifested in changed mechanical properties, including static bending strength and static elastic modulus. Modulus of elasticity is a very important parameter to judge the strength performance of composites. The width and the thickness of CFRWCs samples were measured using a vernier caliper at 20 °C, the precision of which was 0.01 mm. After that, the samples were fully pressed by universal mechanical testing machine. Equation 1 was used to calculate the static bending strength σ_b (MPa) :

$$\sigma_b = \frac{3lP_{\max}}{2bh^2} \tag{1}$$

where P_{max} is maximum load (N), l is the distance between two support of machine (mm), b is the specimen width (mm), and h is the specimen thickness (mm). Static elastic modulus E (Mpa) was calculated using Eq. 2,

$$E = \frac{l^3}{4bh^3} \times \frac{\Delta f}{\Delta s} \tag{2}$$

where l is the distance between two support of machine (mm), b is the specimen width (mm), h is the specimen thickness (mm), Δf is increment of internal force (N), and Δs is the deformation amount (mm).

Measurement of surface resistance

Surface resistances of CFRWCs samples were measured in two conditions by an intelligent resistance tester (Model SB2230; Shanghai Dual Electric Instruments Co. Ltd., China). Compared with pole-pole method, the four-electrode method can measure data more precisely and eliminate both electrode resistance and contact resistance (Zhou *et al.* 2011). In the first condition, the surface resistance of each sample was measured at 20 °C. Due to an uneven distribution of carbon fibers, three spots were selected randomly to measure surface resistances and then the average value was calculated for each side. In the second condition, all the samples were put into a constant temperature drying box (WGL-65B; Hangzhou Aipu Instrument & Equipment Co. Ltd., China) with a temperature range of 0 to 300 °C for 30 min. Different temperatures were set on the drying box to change the inside temperature from 20 °C to 120 °C. Data were collected after the temperature of the samples was stable in different temperature environments. Surface resistivity ρ (Ω/cm) of CFRWCs was calculated using Eq. 3,

$$\rho = \frac{RS}{L} \tag{3}$$

where R is the surface resistance (Ω), L is the specimen length (mm), and S is the cross-sectional area (m^2). The voltage distributions of CFRWCs samples were simulated using a finite element analysis software (ANSYS 14.0; ANSYS, Inc., USA). The models of specimens were established in the electrical environment of ANSYS, whose parameters could be also set, such as the area, the voltage and the relative permittivity. Then the simulated images were shown in the software. Not only that, ANSYS could also simulate CFRWCs samples in the microcosmic field, like π bonds of carbon fibers.

Measurement of dielectric constant and loss tangent

After the measurement of surface resistances, the diameter and the thickness of samples were manufactured to be 50 mm and 4 mm, respectively. In order to remove the remaining moisture content in the CFRWCs, samples were dried in an air oven at 45 °C for 12 h. The dielectric constant and the loss tangent of each sample were analyzed using a dielectric constant tester (NS238A; Agilent Technologies, USA), the frequency of which was from 7 GHz to 18 GHz at 20 °C. The dielectric constant tester showed five values for each sample at different frequencies, which was beneficial to study the dielectric constants of CFRWCs. The capacitance C (F) of CFRWCs was calculated using Eq. 4,

$$\varepsilon = \frac{Ct}{\varepsilon_0 A} \tag{4}$$

where t is the specimen thickness (mm), A is the specimen area (m^2), ε is the dielectric constant (F/m), and ε_0 is the permittivity of free space (F/m), the value of which is 8.854×10^{-12} F/m.

Preparation of specimens for scanning electron microscopy

Scanning electron microscopy (SEM) is an effective method to investigate composites in the microcosmic field. The length and the thickness of the CFRWCs samples were required to make 30 mm by 30 mm and 4 mm, respectively. After that, the specimens were stuck on the base of SEM using conductive tape. Due to the insulation of the composites, the specimens were coated with a layer of conducting film before observation. The SEM was selected from Phenom-World Co., Ltd. (Holland), the model of which was Phenom Pro.

RESULTS AND DISCUSSION

Enhanced Mechanical Properties

Table 2 reveals that the mechanical properties of CFRWCs samples had been strengthened by the reinforcement, in comparison with crude wood sample 31#.

Table 2. Enhanced Mechanical Properties of CFRWCs

Sample	Maximum Load (N)	Static Bending Strength (MPa)	Static Elastic Modulus (MPa)
11#	1169.03	16.17	2436.83
12#	1394.19	19.02	3082.84
13#	1627.20	22.63	3957.55
21#	1504.12	20.94	3502.54
22#	1660.93	23.97	4135.10
23#	1823.72	27.61	5078.56
31#	815.54	12.66	1798.05

This is reasonable in view of the fact that the modulus of carbon fiber is about 230 GPa (Qi *et al*. 2003), which is very much higher than that of wood fiber, and it shows that carbon fibers can reinforce the mechanical properties of composites (Kim *et al*. 2009). It is also obvious that the maximum load, the static bending strength, and the static elastic modulus of a two-sided sample generally outweigh those of a single-sided sample when the carbon fiber content is equal.

Impact of Carbon Fiber Content

The experimental temperature and the frequency were set as 20 °C and 10^4 Hz, respectively. The electrical properties of CFRWCs samples, which include dielectric constant, capacitance, loss tangent, and surface resistivity, are presented in Table 3. Results shown for samples $11^{\#}$, $12^{\#}$, and $13^{\#}$ show that the dielectric constants and the capacitances increased with increasing carbon fiber content from 55 wt.% to 75 wt.%. On the contrary, the loss tangents and the surface resistivities decreased as carbon fiber content was increased continuously. The trend of $21^{\#}$, $22^{\#}$, and $23^{\#}$ was similar to that observed for $11^{\#}$, $12^{\#}$, and $13^{\#}$. It is apparent by comparing $11^{\#}$ and $21^{\#}$ that the loss tangents and the surface resistivities of two-sided CFRWCs samples were lower than those of single-sided CFRWCs samples. However, the dielectric constants and the capacitances of two-sided CFRWCs samples exceeded those of single-sided CFRWCs samples.

Table 3. Electrical Parameters of CFRWCs

Sample	Dielectric Constant (F/m)	Capacitance (F)	Loss Tangent (%)	Surface Resistivity (Ω/cm)
$11^{\#}$	2.78	1.21×10^{-11}	2.59×10^{-2}	16.13
$12^{\#}$	3.34	1.45×10^{-11}	2.37×10^{-2}	13.81
$13^{\#}$	6.16	2.67×10^{-11}	1.46×10^{-2}	9.87
$21^{\#}$	3.47	1.51×10^{-11}	2.41×10^{-2}	13.71
$22^{\#}$	4.31	1.87×10^{-11}	1.98×10^{-2}	10.31
$23^{\#}$	8.20	3.57×10^{-11}	1.12×10^{-2}	5.25

From the perspective of macroscopic field, the data for samples $11^{\#}$, $12^{\#}$, and $13^{\#}$ show this trend, which is due to the fact that carbon fibers have good electrical conductivity. They enabled the dielectric constant of composites to increase rapidly and controlled the surface resistivity no more than 16.13Ω/cm. As a result, The conduction of electricity of all of the whole CFRWCs samples was improved by adding carbon fiber content from 55 wt.% to 75 wt.%.

Figure 2 shows simulation of the voltage distribution of CFRWCs $11^{\#}$ in the macroscopic field. In the modeling, the 55 wt.% carbon fibers were assumed to have uniformly distribution on the surface. The dielectric constant of $11^{\#}$ was set as 2.78 F/m in the material model, whose size was modeled as 10 cm × 5 cm. Then the voltage of the bottom side was set as 0 v, while the midpoint of the top side was loaded 220 v. As shown in the figure, the voltage distribution appeared as a stair-step shape. Different colors represented different ranges of value, which showed that there is an electric potential difference on the surface and thus proved CFRWCs could conduct electricity.

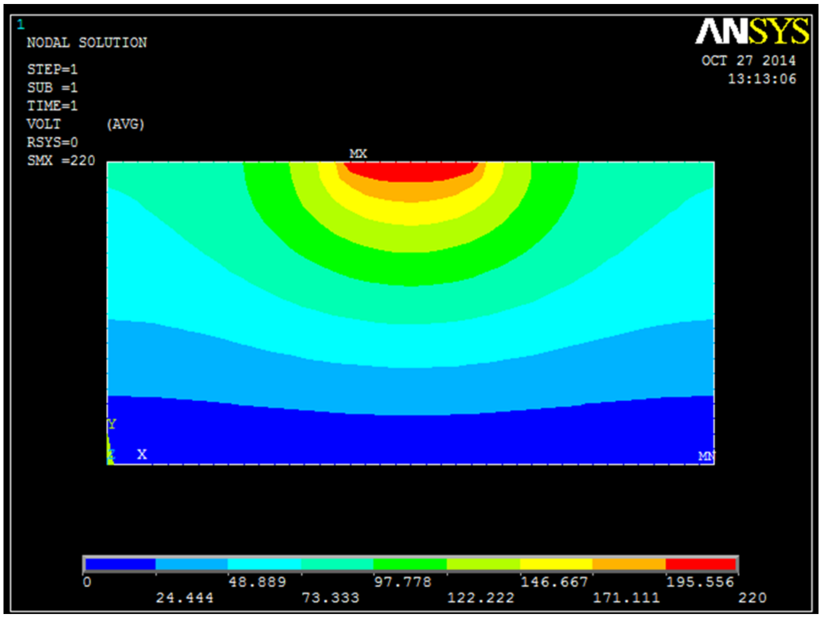

Fig. 2. Simulated image of voltage distribution of CFRWCs 11# in the macroscopic field

From the perspective of the microcosmic field, the presence of electron holes is the primary way for carbon fibers to conduct electricity. Some valence electrons of carbon fibers get some energy and get rid of the constraint of covalent bonds due to the thermal motion. At the same time, they leave vacancies in the covalent bonds. After that, the adjacent electrons will fill the vacancies and then leave new ones, which result in the charge migration in the covalent bonds as well as hole conduction. Besides, aromatic rings of carbon fibers form a conjugated system. The movement of π electrons can cause electric conduction in the composites as well. The number of π electrons is increasing when adding more carbon fibers into the CFRWCs samples so that the electrical conductivities are enhanced. A simulated image of π bonds is shown in Fig. 3.

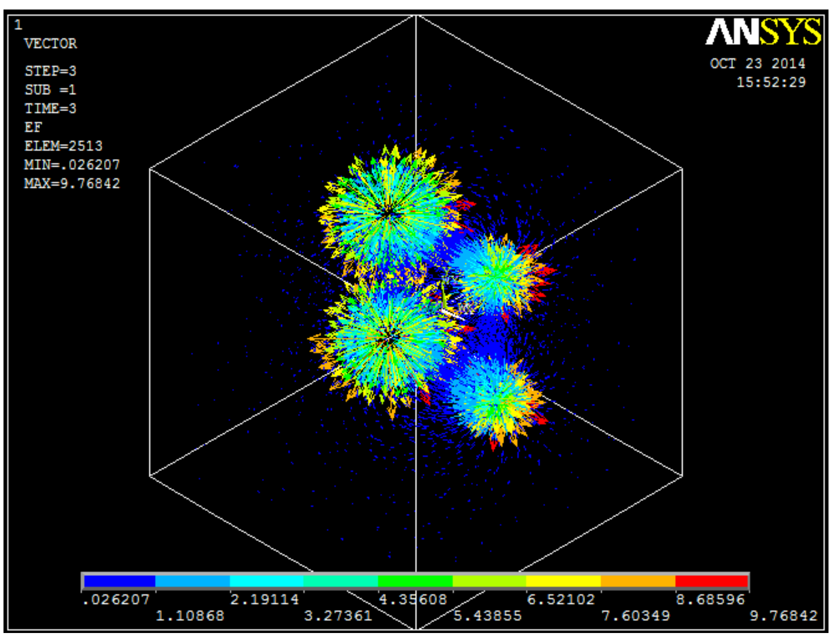

Fig. 3. Simulated image of π bonds of carbon fibers

As shown in this figure, π bonds presented a mirror symmetry of electron clouds. Electron clouds were assumed as ellipsoids or spheres because the moving tracks of extranuclear electrons were uncertain, but they were symmetrically distributed. Different colors indicates the probability of the emergence of electrons. The blue one represents the lowest percentage, as well as the lowest quantity of electric charge. Meanwhile, the lowest quantity of electric charge was assigned 2.62×10^{-2}c. The other ones represent various quantities of electric charges, which changed with colors. The π electron clouds were located on both sides, rather than gathered on a nucleus. Such a space structure reduced the binding force of a nucleus and enabled the electrons be more active.

The SEM micrographs of CFRWCs samples, which include 55 wt.% carbon fibers, 65 wt.% carbon fibers, and 75 wt.% carbon fibers, are displayed in Figs. 4a, 4b, and 4c, respectively.

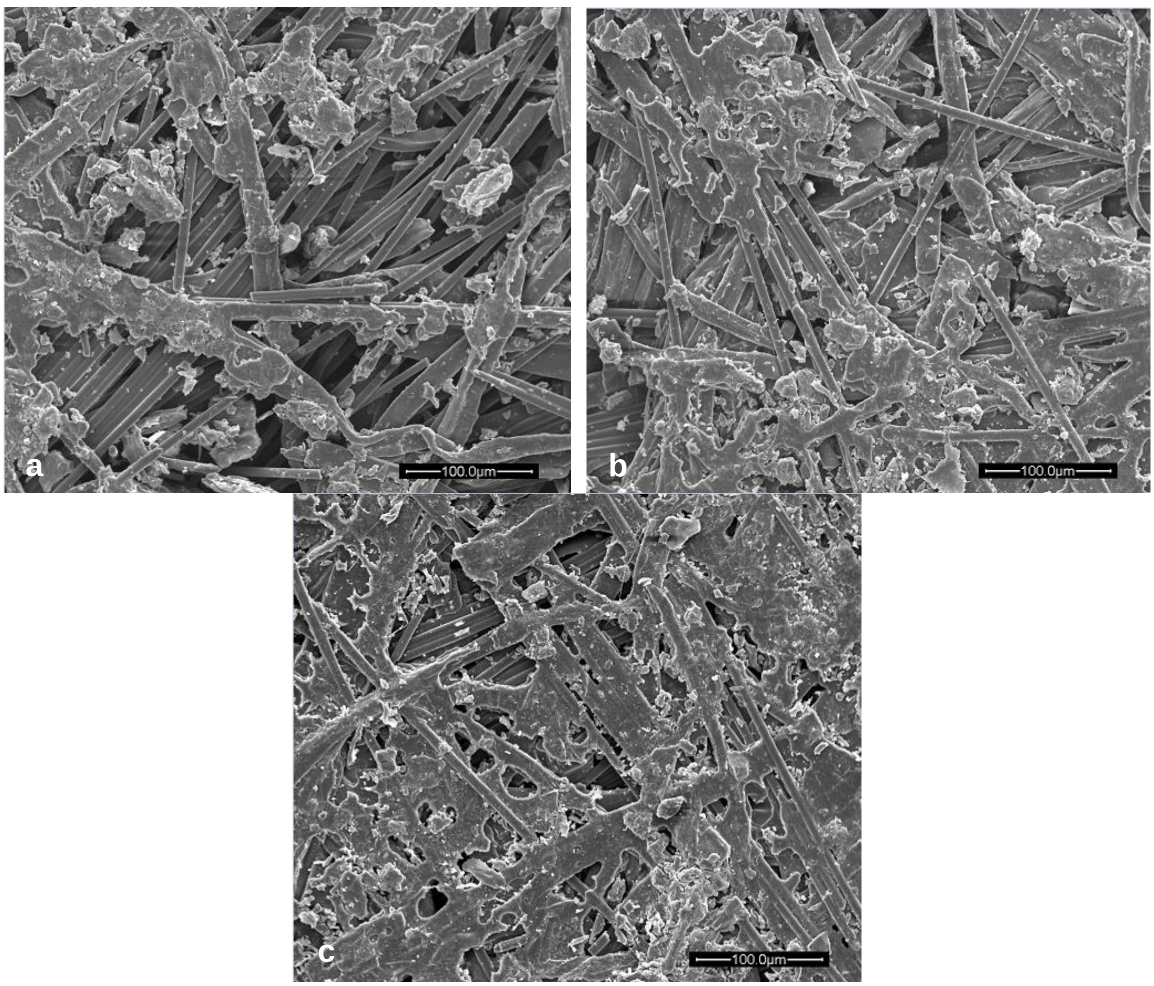

Fig. 4. SEM micrographs of CFRWCs samples containing (a) 55 wt.% carbon fibers; (b) 65 wt.% carbon fibers; and (c) 75 wt.% carbon fibers

As shown in these figures, the main component of CFRWCs was carbon fibers with different content, which were distributed uniformly on the surface. Well-distributed carbon fibers on the surface were crucial, and they determined the measurement results. Compared with Fig. 4a, the degree of carbon coverage of Fig. 4b was more intensive, which meant that the conductive grid was larger and conductive particles contacted closer.

They were beneficial to create a current and then conduct electricity. In this research, the conductivity mainly depended on conductive material concentration. The higher the percentage of carbon fiber, the lower value of resistance. This further demonstrated that Fig. 4c with 75 wt.% carbon fibers had the best electrical properties among them.

From the perspective of a mesoscopic field, the number of conductive paths on the surface of CFRWCs increases and conductive grid expands as carbon fiber content is increased. When carbon fiber content reaches and is over 30 wt.%, a large part of the conductive paths are connected in the composites (Wang 2014). Some conductive particles form a conductive network in the composites, but the other isolated conductive particles cannot do this. However, when the distance between two isolated conductive particles is less than 10 nm, then a channel current can be formed under the effect of an external electric field. Comparing $11^{\#}$ with $21^{\#}$ in the mesoscopic field, it is apparent that the electrical conductivity of a two-sided sample was higher than that of a single-sided sample. The conductive network of a two-sided sample is larger, and it can conduct electricity on both sides.

Impact of Sample Temperature

Table 4 shows the surface resistivities of all the samples of CFRWCs at different temperatures. The samples had been put into the constant temperature drying box for 30 min to warm up.

Table 4. Surface Resistivities of CFRWCs at Different Temperatures

Temperature (°C)	Surface Resistivity (Ω/cm)					
	$11^{\#}$	$12^{\#}$	$13^{\#}$	$21^{\#}$	$22^{\#}$	$23^{\#}$
20	16.13	13.81	9.87	13.71	10.13	5.25
30	12.45	9.44	6.65	10.02	6.59	3.38
40	9.84	6.25	4.03	6.75	5.54	2.46
50	6.46	4.54	2.90	5.24	3.67	2.30
60	5.11	3.68	2.68	4.53	3.08	1.98
70	4.15	2.97	2.35	3.68	2.65	1.67
80	3.93	2.79	2.17	2.97	2.26	1.56
90	3.52	2.51	1.96	2.84	1.91	1.43
100	3.22	2.30	1.65	2.49	1.67	1.44
110	3.05	2.22	1.58	2.38	1.62	1.42
120	2.95	2.14	1.51	2.30	1.61	1.42

Values obtained for $11^{\#}$, $12^{\#}$, and $13^{\#}$ illustrate that the surface resistivities decreased with increasing of the temperature from 20 °C to 120 °C. The surface resistivity of crude wood fiber can be regarded as infinity, which means that crude wood fiber can be regarded as an insulator without conducing electricity (Zhang *et al*. 2011). The trend for $21^{\#}$, $22^{\#}$, and $23^{\#}$ was similar to that observed for $11^{\#}$, $12^{\#}$, and $13^{\#}$.

The surface resistivities are compared in Figs. 5 and 6 for CFRWCs samples with raising temperature. Data 1, Data 2, and Data 3 represent 55 wt.%, 65 wt.%, and 75 wt.% carbon fibers, respectively. The curves of single-sided CFRWCs were generally higher than those of double-sided CFRWCs. In Fig. 5, the surface resistivities of single-sided

CFRWCs samples declined rapidly when the temperature was raised from 20 °C to 50 °C, showing a greater rate of change than the others. The rate of change then decreased gradually with increasing temperature to 90 °C. When the temperature was over 90 °C, the attenuation amplitude approached zero, and the surface resistivities reached their minimum. The curves in Fig. 6 show the same trend.

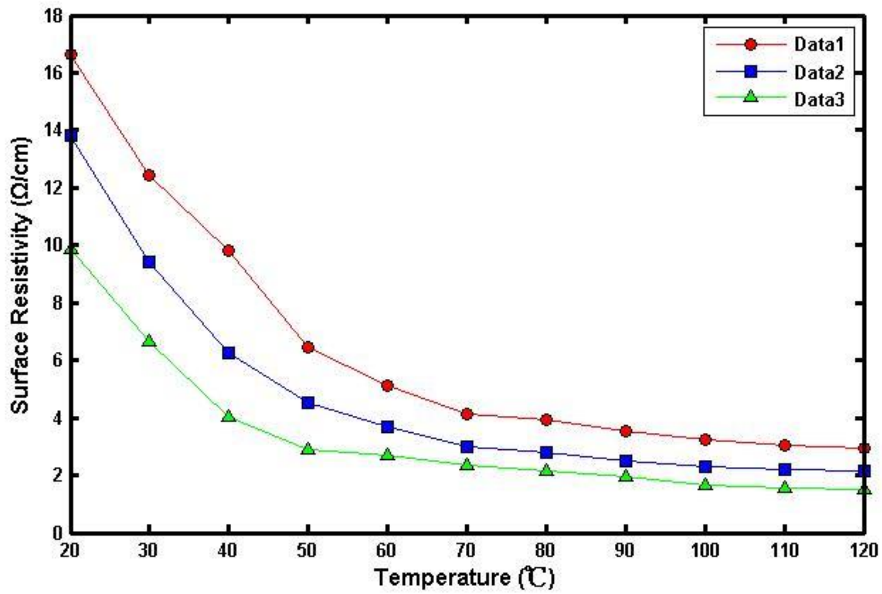

Fig. 5. Curves of surface resistivities of single-sided samples of CFRWCs with 55 wt.% (Data 1), 65 wt.% (Data 2), and 75 wt.% (Data 3) carbon fibers

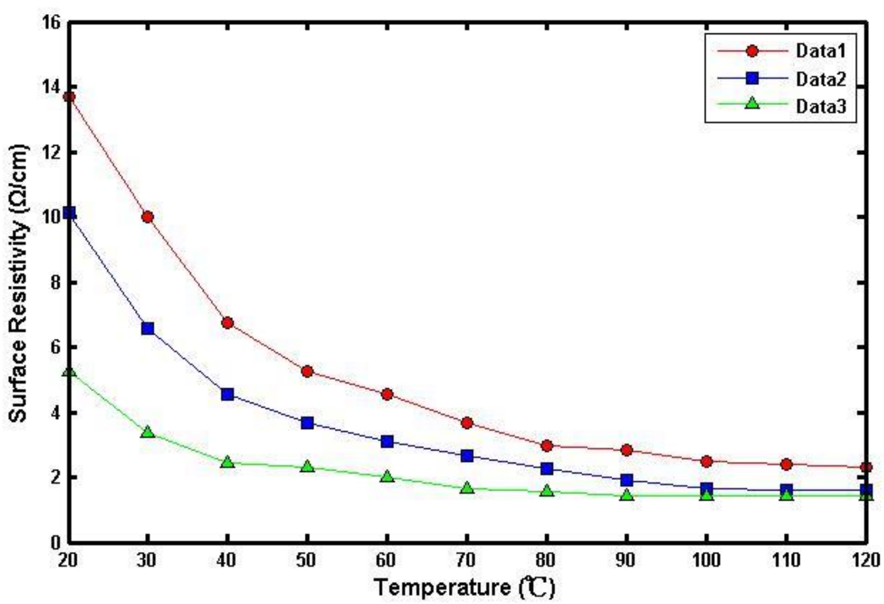

Fig. 6. Curves of surface resistivities of two-sided samples of CFRWCs with 55 wt.% (Data 1), 65 wt.% (Data 2), and 75 wt.% (Data 3) carbon fibers

From the perspective of the macroscopic field, the curves of 11#, 12#, and 13# illustrate that CFRWCs exhibited an NTC effect, whose electrical conductivity is influenced by temperature. The NTC effect corresponds to thermal activation conduction mechanism, which means that thermal resistance decreases with increasing temperature (Sha *et al*. 2004). From the perspective of quantum theory, CFRWCs exhibit a quantum tunneling effect. The energy bands of carbon fiber atoms consist of conduction bands and valence bands. Electrons can conduct electricity and move freely in the conduction band, while they cannot conduct electricity in the valence band. When electrons are motivated by temperature rise in the valence band, they will jump to the conduction band, which is a high energy level. As a result, raising temperature enables electrons to gain more kinetic energy, which promotes the collision of conducting particles (Zhang *et al*. 2013). The jumping electrons increase and form current carriers to conduct electricity, then the surface resistivities of CFRWCs samples decline.

With respect to 11#, the whole attenuation amplitudes of surface resistivity of CFRWCs diminish from 16.13 to 2.95 in the process of raising temperature. The electrons of CFRWCs are in the critical position of excitation when the temperature is under 50 °C. A slight rise in temperature can motivate a large number of electrons. The surface resistivity decreases sharply at the macro level. At the range of 50 to 90 °C, the number of new excited electrons is lower than that of critical position. When the temperature is over 90 °C, the excited electrons of CFRWCs generally reach saturation point, and the current circuits reach the maximum. The surface resistivity flattens at the macro level.

Due to the wave reflection and spurious effect of the multi-scale method, atomic dynamics should be applied to the analytic technique to improve the multiscale method. Multiscale method can be used to study materials on the microscopic scale (Lu *et al*. 2008). In the process of modeling, composites are generally divided into an atomic region, a transitional region, and a continuous finite-element region. However, some high-frequency waves are reflected back, which cannot transmit directly from the atomic region to finite-element region. By modeling with atomic dynamics, the unit length of finite-element region is equal to the distance between adjacent atoms when it is near the transitional region. That makes sure the waves from the atomic region can be transmitted into the finite-element region, and eliminates wave reflection.

CONCLUSIONS

1. The mechanical properties of polar wood panels could be obviously reinforced by adding high percentage of carbon fiber (55 wt.% or above) on the surface of CFRWCs at 20 °C. The maximum load and the static elastic modulus of all the test samples were increased to more than 1100 N and above 2400 MPa, respectively. Static bending strength was enhanced from 12.66 MPa to over 16.17 MPa.
2. Carbon fiber content and temperature were two main factors causing the changes of electrical properties of the CFRWCs. In this research, the reinforced electrical properties were modeled and analyzed using a multiscale method, including from the microcosmic angle, from the mesoscopic view, and from the microcosmic field.

3. The migration of electron holes and the movement of π electrons were two major reasons, which led to the improvement of electrical properties with increasing carbon fiber content from 55 wt.% to 75 wt.%. Under this circumstance, the dielectric constants and the capacitances of CFRWCs rose at 20 °C and 10^4 Hz. An opposite trend was observed in the loss tangents and the surface resistivities.
4. The conductive properties of CFRWCs were improved as the temperature rose from 20 °C to 120 °C. The increasing temperature motivated more electrons to conduct electricity and caused the surface resistivities to decrease. The CFRWCs exhibited an NTC effect as a whole.
5. The attenuation amplitude of surface resistivities was reduced in the process of temperature rise, which resulted in a rapid drop when the temperature was raised from 20 °C to 50 °C and decreased gradually with increasing temperature to 90 °C. It approached zero as the temperature was over 90 °C.
6. Under the same conditions, conductive properties of two-sided CFRWCs are generally better than those of single-sided CFRWCs.

ACKNOWLEDGMENTS

The work reported in this paper was funded by the Natural Science Foundation of Heilongjiang Province, China (No: C201230).

REFERENCES CITED

Alexopoulos, N. D., Bartholome, C., Poulin, P., and Marioli-Riga, Z. (2010). "Damage detection of glass fiber reinforced composites using embedded PVA-carbon nanotube (CNT) fibers," *Compos. Sci. Technol.* 70(12), 1733-1774. DOI: 10.1016/j.compscitech.2010.07.004

Al-Saleh, M. H., and Sundararaj, U. (2011). "Review of the mechanical properties of carbon nanofiber/polymer composites," *Compos Part A: Appl Sci Manuf.* 42(12), 2126-2168. DOI: 10.1016/j.compositesa.2011.08.005

Al-Saleh, M. H., Gelves, G. A., and Sundararaj, U. (2013). "Carbon nanofiber/ polyethylene nanocomposite: Processing behavior, microstructure and electrical properties," *Mater Des.* 52, 128-33. DOI: 10.1016/j.matdes.2013.05.038

Bal, S. (2010). "Experimental study of mechanical and electrical properties of carbon nanofiber/epoxy composites," *Mater Des.* 31(13), 2406-2419. DOI: 10.1016/j.matdes.2009.11.058

Chawla, S., Naraghi, M., and Davoudi, A. (2013). "Effect of twist and porosity on the electrical conductivity of carbon nanofiber yarns," *Nanotechnology* 24(25), 255708. DOI: 10.1088/0957-4484/24/25/255708

Chen, Y. M., and Ting, J. M. (2002). "Ultra high thermal conductivity polymer composites," *Carbon.* 40(3), 359-362. DOI: 10.1016/S0008-6223(01)00112-9

Diao, X. M., and Sun, P. (1993). "Electrical properties of wood and the use of electrical measuring moisture meter," *Wood Processing Machinery* 3, 18-20.

Gui, H. J. (2011). *SCFRW Homogenization Model Based on Digital Image Processing Research*, Master's Thesis, Northeast Forestry University, Harbin.

He, F. (2010). "Carbon fibre composite," in: *Textbook of Carbon Fibers and Graphite Fibers,* F. He (ed.), Chemical Industrial Press, Beijing, pg. 286.

Khan, T. A., Gupta, A., Jamari, S. S., Jose, R., Nasir, M., and Kumar, A. (2013). "Synthesis and characterization of carbon fibers and their application in wood composites," *BioResources* 8(3), 4171-4184. DOI: 10.15376/biores.8.3.4171-4184

Kim, M., Park, Y. B., Okoli, O. I., and Zhang, C. (2009). "Processing, characterization, and modeling of carbon nanotube-reinforced multiscale composites," *Compos. Sci. Technol.* 69(3-4), 335-342. DOI: 10.1016/j.compscitech.2008.10.019

Lee, G. Z. (2010). "Research progress of wood composites," *Wood Processing Machinery* 21(1), 42-45.

Lee, S. B., Choi, O., Lee, W., Yi, J. W., Kim, B. S., and Byum, J. H. (2011). "Processing and characterization of multi-scale hybrid composites reinforced with nanoscale carbon reinforcements and carbon fibers," *Composites Part A* 42(4), 337-381. DOI: 10.1016/j.compositesa.2010.10.016

Lu, X. Z., Lin, X. C., and Ye, L. P. (2008). "Multiscale finite element modeling and its application," *J. of HUST. (Urban Science Edition).* 25(4), 76-80.

Poveda, R., Achar, S., and Gupta, N. (2012). "Thermal expansion of carbon nanofiber-reinforced multiscale polymer composites," *JOM* 64, 1148-1205. DOI: 10.1007/s11837-012-0402-5

Poveda, R. L, and Gupta, N. (2014). "Electrical properties of carbon nanofiber reinforced multiscale polymer composites," *Material and Design* 56, 416-422. DOI: 10.1016/j.matdes.2013.11.074

Qi, Z. J., Lin, S. B., and Yu, Z. H. (2003). "Analysis of PAN-based carbon fiber strength's influencing factors," *Hi-Tech Fiber & Application* 28(4), 30-35.

Rodriguez, A. J., Guzman, M. E., Lim, C. S., and Minaie, B. (2011). "Mechanical properties of carbon nanofiber/fiber-reinforced hierarchical polymer composites manufactured with multiscale-reinforcement fabrics," *Carbon* 49(3), 937-948. DOI: 10.1016/j.carbon.2010.10.057

Salinier, A., Dagréou, S., Léonardi, F., Derail, C., and Navascués, N. (2013). "Electrical, rheological and mechanical characterization of multiscale composite materials based on poly(etherimide)/short glass fibers/multiwalled carbon nanotubes," *Composite Structures* 102, 81-89. DOI: 10.1016/j.compstruct.2013.02.025

Sha, Z. Y., Wang, Y. P., and Du, Z. T. (2004). "Linearization and application of NTC thermistor," *Process Automation Instrumentation* 25(9), 28-30.

Wang, Z. J., Li, K. Z., and Wang, C. (2009). "Electricity characteristics of carbon fiber reinforced cement based composites (CFRC)," *Journal of Materials* 23(12), 47-51.

Wang, Z. S. (2014). *Simulation Research on Electromagnetic Shielding Performance of CFRW Based on Finite Element*, Master's Thesis, Northeast Forestry University, Harbin.

Yang, X. P., Rong, H. M., and Lu, Z. D. (2000). "Study on the electrical properties of carbon fiber reinforced conductive composites," *Materials Engineering.* 9, 11-14.

Zhang, D. Y., Kuai, H. J., and Sun, L. P, (2011). "Numerical analysis of electrical conductivity of short carbon fiber reinforced wood," *Journal of Northeast Forestry University* 39(2), 109-111.

Zhang, Y. L., and Wang, Z. S. (2013). "Research on the resistivity-temperature characteristic of carbon fiber reinforced wood composite material," *Development and Application of Materials* 28(6), 34-37.

Zhou, M., Wang, J. G., and Huang, S. B. (2011). "Experimental investigation on influencing factors in soil resistivity measurement," *Rock and Soil Mechanics* 32(11), 3269-3275.

Article submitted: December 12, 2014; Peer review completed: February 9, 2015; Revised version received and accepted: February 20, 2015; Published: February 27, 2015.
DOI: 10.15376/biores.10.2.2392-2405